CompBat Deliverable

D2.1 Multiphysics redox-flow battery FEM battery model, parametrized by DFT and experimental data and able to reproduce experimental voltage/current data for long-term battery operation

Grant Agreement number	875565
Action Acronym	CompBat
Action Title	Computer aided design for next generation flow batteries
Funding Scheme	H2020-LC-BAT-2019
Duration of the project	36 months, 1 February 2020 – 31 January 2023
Work package	WP2 - *Finite element simulations*
Due date of the deliverable	31 July 2021
Actual date of submission	30 September 2021
Lead beneficiary for the deliverable	Uppsala University
Dissemination level of the deliverable	Public

Project coordinator's scientific representative

Dr. Pekka Peljo

Aalto korkeakoulusäätiö, Aalto University (Aalto), School of Chemical Engineering

Department of Chemistry and Materials Science

pekka.peljo@aalto.fi

Authors		
Name	Beneficiary	E-mail
Daniel Brandell	Uppsala University	daniel.brandell@kemi.uu.se
Alexis Rucci	Uppsala University	alexis.rucci@kemi.uu.se

Internal QA			
Reviewer	Date of review	Comments	Date of revision
Pekka Peljo	30.09.2021	OK	

Abstract/Executive summary

Deliverable 2.1 presents the progress in the development of a Multiphysics redox flow battery model using finite elements methodology. This model has been generated in task 2.1 and parameterized in task 2.2.

The model here presented was developed using the software COMSOL Multiphysics® and considering two different approaches: pseudo stationary and time dependent. The main advantage of the first one is the low computational cost and it was used for the optimization routines and calculation of polarization curves. On the other hand, the development of the transient model was carried out in order to create a predictive tool able to estimate the voltage and current production.

Results here presented were compared with experimental measurements for all-vanadium redox flow batteries and will be extended to other redox couples.

Contents

Contents

The CompBat project focuses on developing tools for discovery of new prospective candidates for next generation of redox flow batteries (RFB). Numerical modelling with finite element method (FEM) is necessary to estimate the cell performance, identifying the critical points under different scenarios. This development is carried out within work package WP2.

In the present deliverable, a two-dimensional model for an RFB was constructed, parameterized and validated with experiments. The mathematical approach was based on the diluted concentration theory, considering charge conservation and Nernst-Planck transport equation. Two different models were investigated, a pseudo steady-state and transient models. In the first one, all the variables are calculated at a certain state of charge (SOC) and the cell behaviour is represented with a sweep of all the SOC. In the second study, the RFB representation was coupled to a laminar flow and 0D tank models and all the variables are time dependent.

Within this context, the mathematical equations for both cases (pseudo steady-state and transient) are described together with the parametric sweep carried out during the model development. Results for polarization and charge-discharge curves were compared with experimental measurements and, in addition, all the results have been analysed identifying the main causes of discrepancies.

1   Pseudo steady state model

The proposed model was implemented following the architecture of an all-vanadium redox flow battery. Positive and negative electrolytes are a sulfuric acid solution containing vanadium ions, which are stored in respective tanks and circulated to the battery cell. The

reactions occurring in the battery cell during charge-discharge cycles are represented in the following equations:

Positive electrode: $VO^{2+} + H_2O - e^- \rightleftharpoons VO_2^+ + 2H^+$

Negative electrode: $V^{3+} + e^- \rightleftharpoons V^{2+}$
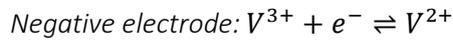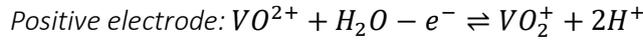
For the construction of the computational model the commercial FEM software COMSOL Multiphysics® was used. On the other hand, the geometry for the battery cell was developed in a 2D representation. The battery consists of two half cells of carbon felt with a Nafion membrane. The current collectors, inlets and outlets were defined as boundaries conditions. The scheme of the implemented geometry is depicted in figure 1.
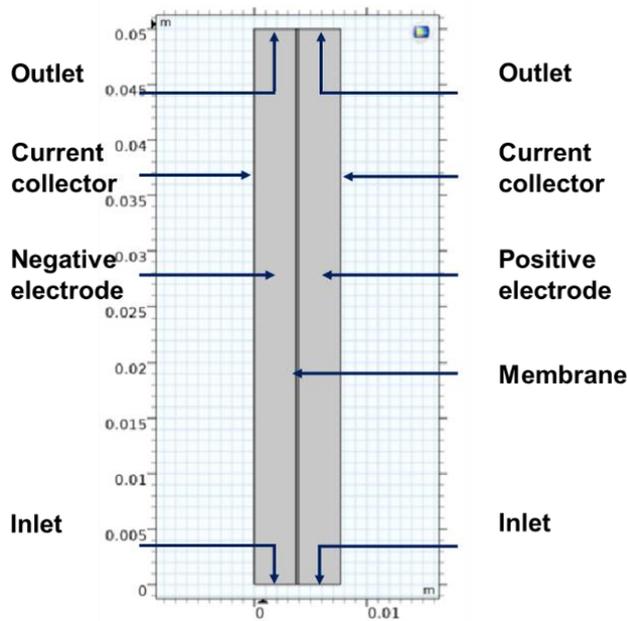
Figure 1. Representation of the 2D geometry implemented in this model.

1.1   Mathematical model.

In this model it was assumed the applicability of transport equations in dilute solutions,[1] the molar flux, *Nj*, of ionic species *j* in a porous medium of porosity ϵ can be expressed via a modified Nernst-Planck equation as:

$$N_j = C_j v - \frac{z_j C_j D_j^{eff} F}{RT} \nabla \phi_e - D_j^{eff} \nabla C_j$$

Where C_j is the concentration of species j, ϕ_e is the electric potential in the electrolyte, $\boldsymbol{v}$ is the velocity of the electrolyte, z_j the charge number for species j and D_j^{eff} is the effective diffusion coefficient, related to the usual diffusion coefficient by the Bruggeman relation: $D_j^{eff} = \epsilon^{3/2} D_j$. The terms in the equation represent ionic transport due to convection, electrokinetic effects and the hydrodynamic dispersion. The volume-averaged differential material balance in the electrode for species j is expressed as:

$$\frac{\partial}{\partial t}(\epsilon C_j) + \nabla \cdot \boldsymbol{N}_j = -S_j$$

Where S_j is the source term for species j. These terms depend of the electrochemical reaction on the surface of both positive and negative porous electrodes represented by the Butler-Volmer law.

On the other hand, the electrolyte is assumed electroneutral, i.e.,

$$\sum_j z_j C_j = 0$$

Expressions for the transfer current densities are:

$$j_1 = Fk_1 \left(C_{VO^{2+}}\right)^{\alpha_{1,c}} \left(C_{VO_2^+}\right)^{\alpha_{1,a}} \left[\frac{C_{VO^{2+}}^s}{C_{VO^{2+}}} exp\left(\frac{\alpha_{1,a}F\eta_1}{RT}\right) - \frac{C_{VO_2^+}^s}{C_{VO_2^+}} exp\left(-\frac{\alpha_{1,c}F\eta_1}{RT}\right)\right]$$

$$j_2 = i_2^0 = Fk_2 \left(C_{V^{2+}}\right)^{\alpha_{2,c}} \left(C_{VO^{3+}}\right)^{\alpha_{2,a}} \left[\frac{C_{V^{2+}}^s}{C_{V^{2+}}} exp\left(\frac{\alpha_{2,a}F\eta_2}{RT}\right) - \frac{C_{V^{3+}}^s}{C_{V^{3+}}} exp\left(-\frac{\alpha_{2,c}F\eta_2}{RT}\right)\right]$$

Where k is the standard reaction rate constant, $\alpha_{i,a}$ the anodic transfer coefficient, $\alpha_{i,c}$ the cathodic transfer coefficient and η_i the over-potential defined for positive and negative as:

$$\eta_1 = \phi_s - \phi_l - U_1$$
$$\eta_2 = \phi_s - \phi_l - U_2$$

Where U_1 and U_2 are the open circuit voltage (OCV) for negative and positive electrodes defined by the Nernst equations including the proton activity at the positive half-cell as reported by Chen et al.[2] In addition, due to the difference in proton activities between positive and negative electrodes, a Donnan potential was considered across the membrane.[3]

$$U_1 = U_1^0 + \frac{RT}{F}\ln\left(\frac{C_{VO_2^+} \cdot \left(C_{H^+,1}\right)^2}{C_{VO^{2+}}}\right)$$

$$U_2 = U_2^0 + \frac{RT}{F} \ln\left(\frac{C_{V^{3+}}}{C_{V^{2+}}}\right)$$

$$U_m = \frac{RT}{F} \ln\left(\frac{C_{H^+,1}}{C_{H^+,2}}\right)$$

Charge balance equations are determined by Ohm's law

$$\nabla\left(-\sigma_s \ \nabla\phi_s\right) = 0$$

In the pseudo steady-state approach, also known as Vynnyckys' model,[2,4,5] all the parameters are stationary. Species concentration at the inlets are set to constants for each SOC, determined by the following set of equations:

$$C_{VO^{2+}}^{in} = C_{V_{total},1}(1 - SOC)$$

$$C_{VO_2^+}^{in} = C_{V_{total},1}SOC$$

$$C_{V^{2+}}^{in} = C_{V_{total},2}SOC$$

$$C_{V^{3+}}^{in} = C_{V_{total},2}(1 - SOC)$$

The relationship between charge or discharge time can be calculated using the expression:

$$SOC = SOC^0 + \frac{t}{t_0}(SOC^f - SOC^0)$$

Where t_0 is the total charge or discharge time. In this model, all the variables are calculated performing a parametric sweep for all the SOCs, obtaining the battery voltage profile and variables calculation without a significant loss of accuracy.

1.2   Simulation parameters.

Tables 1-4 list the main parameters used for the polarization and charge-discharge curves simulations presented in section 4. All these parameters correspond to all-vanadium redox flow batteries and were obtained from experimental setup, parametric sweep and literature.

compbat

Table 1. Electrode properties.

Description	Symbol	Value	Origin
Cell height / m	H	0.05	Experimental setup
Cell depth / m	W	0.04	Experimental setup
Electrode thickness / m	d	0.00375	Experimental setup
Porosity	ε	0.93	Experimental setup
Effective Electronic conductivity / S m^{-1}	σ_e^{eff}	20	Sensitivity analysis

Table 2. Membrane properties.

Description	Symbol	Value	Origin
Area / m^2	A_m	0.002	Experimental setup
Fixed site concentration / mol m^{-3}	c_f	1990	Ref [3,4,6,7]
Charge of fixed site	z_f	-1	Ref [3,4,6,7]
Proton diffusion coefficient / m^2 s^{-1}	D_{H+}	9.312E-09	Ref [3,4,6,7]

Table 3. Electrolyte properties.

Description	Symbol	Value	Origin
Initial vanadium concentration (positive) / mol m^{-3}	c_1^0	1600	Experimental setup
Initial vanadium concentration (negative) / mol m^{-3}	c_2^0	1600	Experimental setup
Initial H$_2$SO$_4$ concentration (positive) / mol m^{-3}	c^0_{H2SO4}	2000	Experimental setup
Proton diffusion coefficient / m^2 s^{-1}	D_{H+}	9.312E-09	Ref [3,4,6,7]
VO^{2+} diffusion coefficient / m^2 s^{-1}	D4	2.0E-9	Sensitivity analysis
VO$_2^+$ diffusion coefficient / m^2 s^{-1}	D5	2.0E-9	Sensitivity analysis
V^{2+} diffusion coefficient / m^2 s^{-1}	D2	2.0E-9	Sensitivity analysis
V^{3+} diffusion coefficient / m^2 s^{-1}	D3	2.0E-9	Sensitivity analysis

Table 4. Kinetic parameters.

Description	Symbol	Value	Origin
Standard reaction rate constant (positive) / m s^{-1}	k_1	1.50E-07	Sensitivity Analysis
Standard reaction rate constant (negative) / m s^{-1}	k_2	1.50E-07	Sensitivity Analysis
Anodic transfer coefficient (positive)	$\alpha_{1,a}$	0.5	Ref [3,4,6,7]
Cathodic transfer coefficient (positive)	$\alpha_{1,c}$	0.5	Ref [3,4,6,7]
Anodic transfer coefficient (negative)	$\alpha_{2,a}$	0.5	Ref [3,4,6,7]
Cathodic transfer coefficient (negative)	$\alpha_{2,c}$	0.5	Ref [3,4,6,7]
Equilibrium potential VO^{2+}/VO_2^+ / V	U_1^0	1.15	Sensitivity Analysis
Equilibrium potential V^{2+}/V^{3+} / V	U_2^0	-0.255	Sensitivity Analysis

2 Transient model

The aforementioned stationary approach demonstrated to be a very good tool for the characterization of the RFB, and, due to the relatively low computational cost, can be used for sensitivity studies and experimental validation without loss of accuracy. Nevertheless, the objective of the project is the development of a computational tool for current and voltage prediction and, in consequence, the most appropriate approach is a time dependent battery model.[8]

The main challenges in a transient study are (i) the coupling of a fluid model with a tank description and time dependent equations for all the vanadium species; (ii) high computational cost and (iii) the model is prone to loss of convergence due to the high sensitivity of the simulation parameters.

In this case, the electrolyte tank for each half cell was represented with a 0D model as follow:[9]

$$\frac{V}{L}\frac{d}{dt}C_{in,i} = \int_{oulet}(\mathbf{N_i}\cdot\hat{\mathbf{n}})dS - \int_{inlet}(\mathbf{N_i}\cdot\hat{\mathbf{n}})dS$$

Where V is the volume of electrolyte and L is the battery 'height' in the 2D representation of figure 1.

On the other hand, the mass balance equation needed to be adapted as follow:

$$\frac{\partial C_i}{\partial t} = D_i^{eff} \nabla^2 C_i + \frac{Fz_i}{RT} \vec{\nabla} \cdot \left(D_i^{eff} C_i \vec{\nabla} \phi_s \right) - \vec{\nabla} \cdot (\vec{v} C_i) + S_i$$

The flux of electrolyte into each half cell is assumed laminar, incompressible and neglecting the gravity effects. Velocity was applied at the inlet and a pressure condition to the outlet. On the other hand, a mapped rectangular mesh and boundary meshing are used to resolve the steep gradients in the electrolyte close to the current collector surfaces. Meshing and velocity fields are depicted in figure 2.
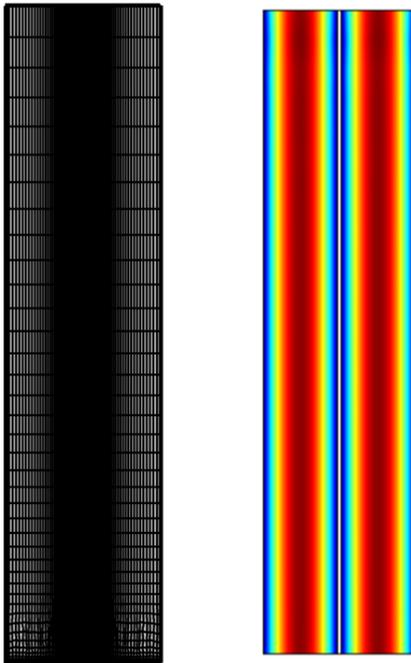
Figure 2. (Left) adaptive rectangular mesh for the battery model and (right) velocity profiles for a laminar flow model.

In addition, all the simulation parameters used in the transient model were the same ones listed in section 2.2.

3   Results and Discussion

The conservation equations were discretized using the module 'Electrochemistry' of the software COMSOL Multiphysics® 5.6. For simulations, a computer with intel® core i9-9980HK CPU @ 2.40GHz 2.40GHz with 32GB of RAM was used.

In this section the results obtained with the developed RFB model are presented and compared with experimental measurements.

3.1 Sensitivity analysis

The parameterization of the model was carried out through a parametric sweep based on the experimental results provided for the all-vanadium flow battery. The most critical parameters were diffusion coefficients, electronic conductivity and equilibrium potential.

Figure 3 depicts the sensibility of the battery voltage performing a parametric sweep of the vanadium species diffusion coefficients. The interval of sweep considered in this study was [1×10^{-7}, 1×10^{-5}] cm^2 s^{-1}.
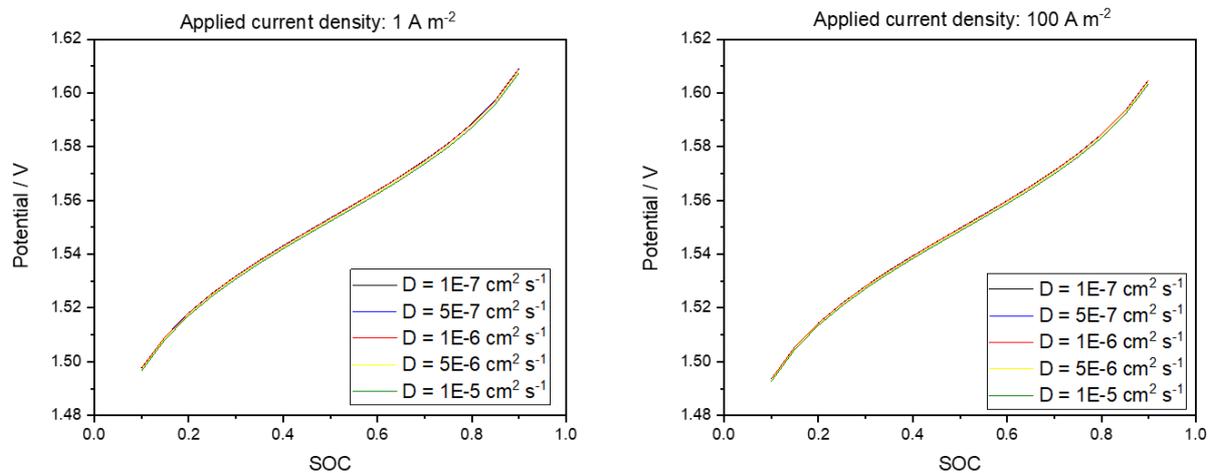
Figure 3. Sensitivity analysis of the pseudo steady-state model considering different diffusion coefficients at low (left) and high current density (right).

Results show that, despite the difference of applied current densities, variabilities in the voltage profiles are negligible and this lack of sensibility reflects a weakness in a pseudo steady-state model implementation. Nonetheless, a higher sensitivity was observed in the calculation of polarization curves. As an example, Figure 4 depicts the change in the polarization curve at SOC = 50% and a flow of 50 ml min^{-1}. In this simulation a combined sweep of the effective electronic conductivity between [10, 1000] S m^{-1} and diffusion coefficients between [1×10^{-7}, 1×10^{-5}] cm^2 s^{-1} was performed. Best values obtained with this sweep were listed in tables 1 and 4.
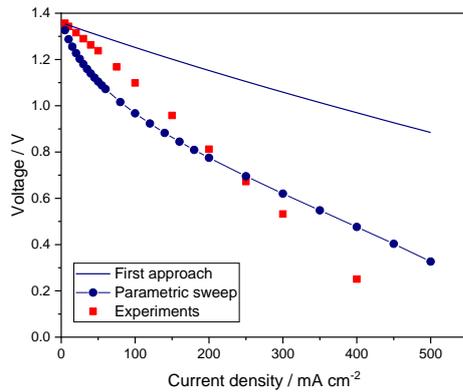
Figure 4. Polarization curves for a vanadium flow battery comparing the experimental values with simulations before and after the combined parametric sweep. Results were obtained at SOC =50% and a flow rate of 50 ml min^{-1}.

3.2   Polarization curves

The validation of the computational model was started with the comparison of polarization curves at different SOC and flow rates with experimental results.

Due to the number of parameters and the complexity of the system, these curves were simulated using the pseudo steady-state model in order to avoid a computational burden. Figure 5 shows the first comparison before the rigorous parametric sweep routine.
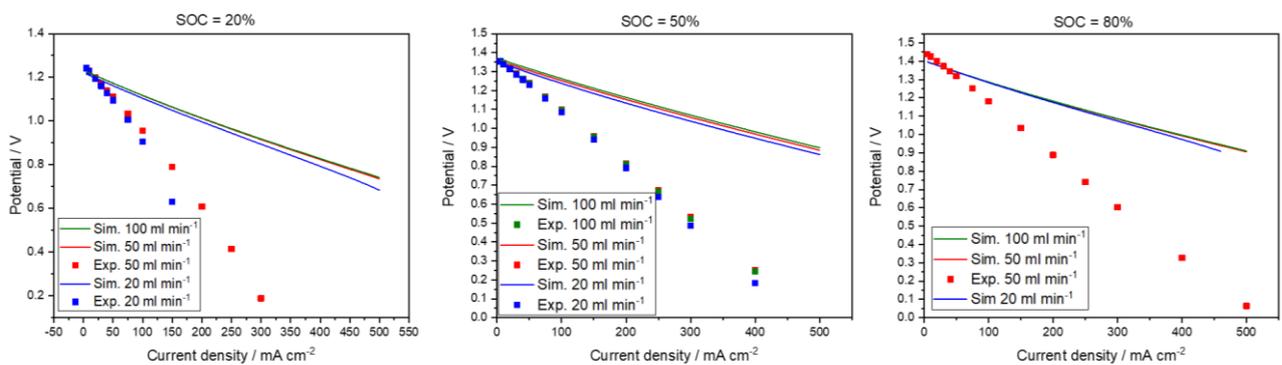
Figure 5. Comparison of experimental and simulation results for polarization curves considering different flow rates before the parametric sweep routine.

Results show a big discrepancy between experiments and simulations. In both cases, ohmic loss dominates the cell behaviour, however the effect of mass transport losses observed in experiments at SOC = 20% is negligible in the simulations. After the sensitivity analysis, results showed an improvement and they are displayed in Figure 6.
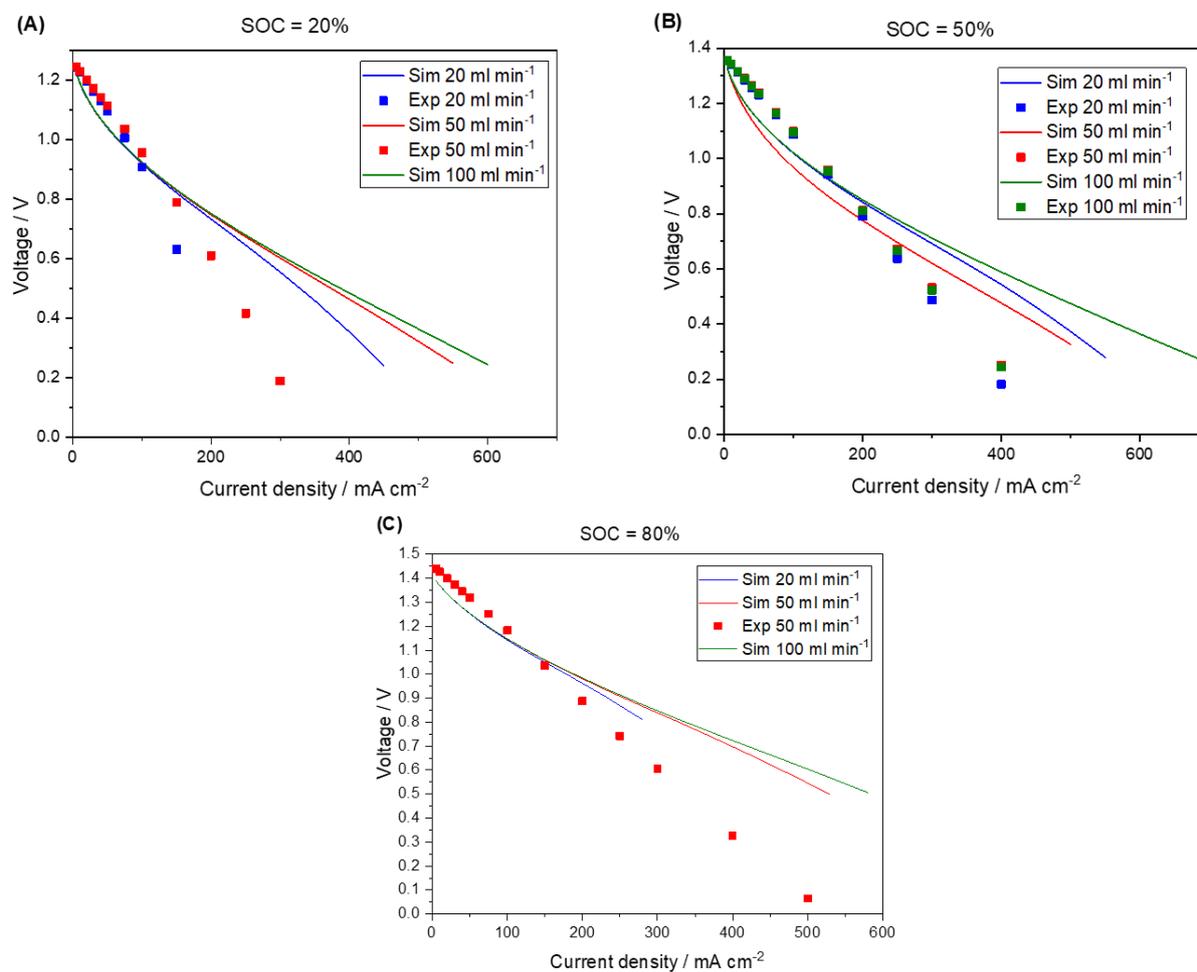
Figure 6. Polarization curves at SOC = 20% (A) 50% (B) and 80% (C) and different flow rates compared with experimental results after the sensitivity analysis.

In this figure, a significant improvement in the slopes of simulated curves is observed. All processes are identifiable, i.e., activation, ohmic and mass transport losses. However, discrepancies are still significant and further optimization is needed. In the experimental results, effects of activation loss are negligible and ohmic and mass transport losses dominate the behaviour. As a first conclusion, an optimization in the kinetic parameters needs to be performed, considering the effect of different reaction rates and exchange current expressions like Tafel equation or linearized Butler-Volmer.[10–12]

3.3   Simulation of Charge – Discharge

The second step in the experimental validation is the simulation of charge-discharge curves for different loading currents. In this case, the transient model was used due to the main objective of the project, i.e., the development of a predictive model for the voltage and current generation of a redox flow battery. The main challenge was the high computational cost due to the coupling of a laminar flow, electrochemical and tank models. Figure 7 shows the comparison between simulations and experiments for a charge-discharge cycle of a vanadium flow battery with a loading current of 50 mA cm^{-2}. Secondly, Figure 8 depicts the voltage profile during charge for a current of 100 mA cm^{-2}
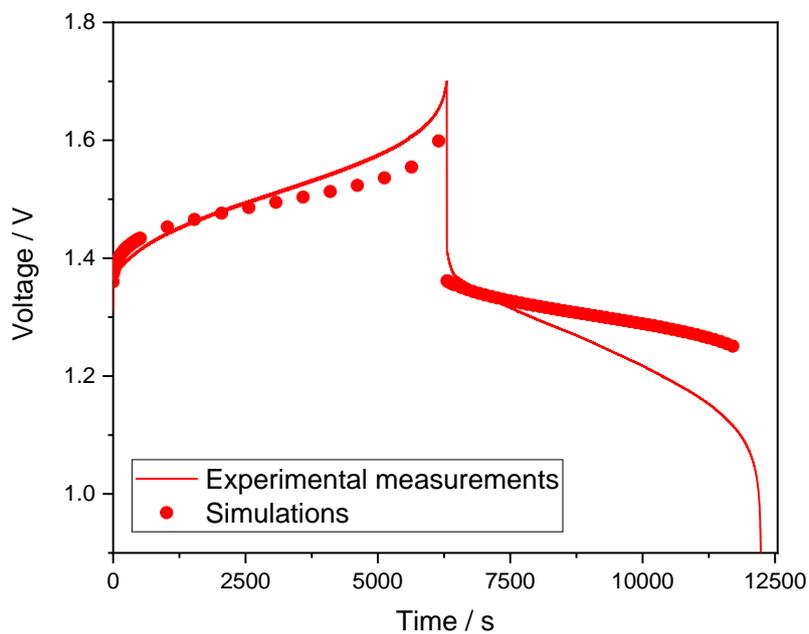
Figure 7. Charge-discharge curve for the all-vanadium system vs time. Comparison between simulation and experimental measurements.
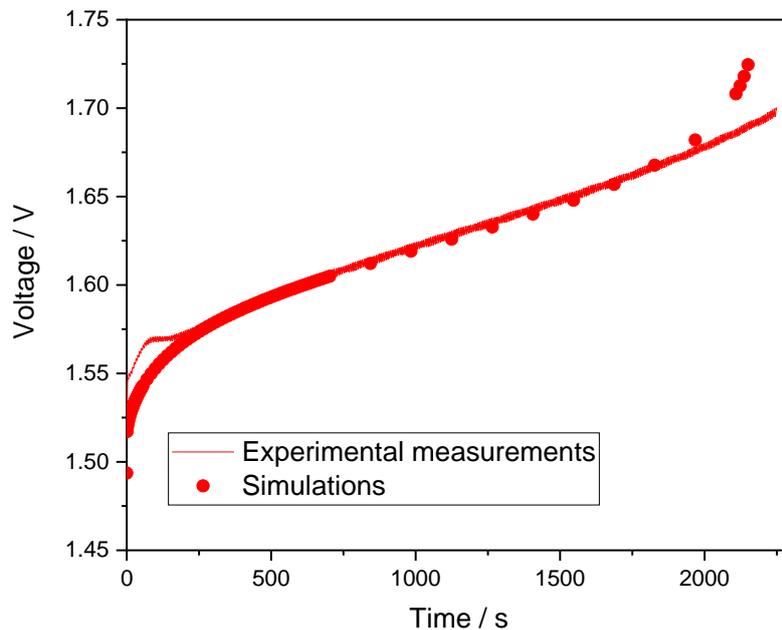
Figure 8. Cell voltage for the all vanadium system during charge and an applied current of 100 mA cm^{-2}. Comparison between simulation and experimental measurements.

In the transient model, the same values of parameters were used. Nonetheless, the influence of time derivative in the mass balance equation and the addition of a 0D model for the tank require another parametric sweep routine in order to fit the experimental and simulated results. Comparison between experiments and simulations in figure 7 shows a significant discrepancy, with an error exceeding the 5%, nevertheless, the model captures the main features of the cell behaviour, predicting the charge and discharge times. These conclusions demonstrate that the conception of the computational model is correct and can be adapted to the system after a rigorous optimization routine. On the other hand, Figure 8 shows a good agreement in both, voltage cut-off and time prediction.

During the charge-discharge cycles, thermodynamic and kinetic factors play different roles depending on the applied current. While the thermodynamic factors dominate the cell performance at low applied currents, kinetic effects are relevant at high currents.[13,14] In the conception of the FEM model, the geometry was simplified to a 2D representation with effective properties for the porous electrode and electrolyte domains. Results in Figure 7 suggest that the electrode and tank properties need to be optimized in order to fit the experimental measurements.

On the other hand, geometrical properties are not relevant at high current and, in consequence, a better agreement between simulation and experiments can be observed.

Nonetheless, further optimization and analysis are needed in order to improve the voltage prediction.

4   Conclusions and prospects

In the present report, a redox flow battery model was developed using finite element methodology. This model was studied into two different approaches: pseudo steady-state and transient considering, in both cases, the Nernst-Planck transport equation for diluted solutions.

A parametric sweep was carried out in order to fit the simulated with experimental values and to obtain the best set of parameters for the model. On the other hand, model validation has been carried out comparing polarization curves and charge-discharge profiles with experimental measurements for all-vanadium flow batteries.

Results presented in this deliverable showed some discrepancies with experimental results, however the main features of the RFBs are captured and the source of these differences has been proved to be related to parameterization.

As a general conclusion, the main objective to this deliverable: '*Development of a Multiphysics redox-flow battery FEM battery model*' was achieved, parameterized both with experimental data and parametric sweep. This model have demonstrated to be able to reproduce the experimental voltage under the correct set of parameters.

Next steps are a further optimization analysis in order to reduce the error between simulation and experiments results and the extension of this model to other redox couples like Fc-Vi and NDI / Fe(CN)6 based redox flow batteries.

5   References

[1]   J. Newman, K. E. Thomas-Alyea, *Electrochemical Systems, 3rd Edition*, Wiley-Interscience, Hoboken, N.J, **2004**.

[2]   C. L. Chen, H. K. Yeoh, M. H. Chakrabarti, *Electrochimica Acta* **2014**, *120*, 167–179.

[3]   K. W. Knehr, E. C. Kumbur, *Electrochem. Commun.* **2011**, *13*, 342–345.

[4]   M. Vynnycky, *Energy* **2011**, *36*, 2242–2256.

[5]   J. Bao, V. Murugesan, C. J. Kamp, Y. Shao, L. Yan, W. Wang, *Adv. Theory Simul.* **2020**, *3*, 1–13.

[6]   M. W. Verbrugge, R. F. Hill, *J. Electrochem. Soc.* **1990**, *137*, 886.

[7]   Y. Y. Choi, S. Kim, S. Kim, J.-I. Choi, *J. Power Sources* **2020**, *450*, 227684.

[8]   B. K. Chakrabarti, E. Kalamaras, A. K. Singh, A. Bertei, J. Rubio-Garcia, V. Yufit, K. M. Tenny, B. Wu, F. Tariq, Y. S. Hajimolana, N. P. Brandon, C. T. J. Low, E. P. L. Roberts, Y.-M. Chiang, F. R. Brushett, *Sustain. Energy Fuels* **2020**, *4*, 5433–5468.

[9]   K. W. Knehr, E. Agar, C. R. Dennison, A. R. Kalidindi, E. C. Kumbur, *J. Electrochem. Soc.* **2012**, *159*, A1446.

[10]   D. Aaron, Z. Tang, A. B. Papandrew, T. A. Zawodzinski, *J. Appl. Electrochem.* **2011**, *41*, 1175.

[11]   C.-N. Sun, F. M. Delnick, D. S. Aaron, A. B. Papandrew, M. M. Mench, T. A. Zawodzinski, *ECS Electrochem. Lett.* **2013**, *2*, A43.

[12]   J. Kim, H. Park, *Renew. Energy* **2019**, *138*, 284–291.

[13]   F. An, L. Chen, J. Huang, J. Zhang, P. Li, *Sci. Rep.* **2016**, *6*, 35051.

[14]   M. Dubarry, G. Baure, C. Pastor-Fernández, T. F. Yu, W. D. Widanage, J. Marco, *J. Energy Storage* **2019**, *21*, 172–185.